Analytical and Bioanalytical Chemistry (2018) 410:7019–7030
https://doi.org/10.1007/s00216-018-1335-9

PAPER IN FOREFRONT

A sample-in-digital-answer-out system for rapid detection and quantitation of infectious pathogens in bodily fluids

Haowen Yang[1,2] · Zhu Chen[3,4] · Xiaobao Cao[1] · Zhiyang Li[5] · Stavros Stavrakis[1] · Jaebum Choo[6] · Andrew J. deMello[1] · Philip D. Howes[1] · Nongyue He[3,4]

Received: 20 June 2018 / Revised: 2 August 2018 / Accepted: 17 August 2018 / Published online: 29 August 2018

Abstract

A variety of automated sample-in-answer-out systems for in vitro molecular diagnostics have been presented and even commercialized. Although efficient in operation, they are incapable of quantifying targets, since quantitation based on analog analytical methods (via standard curve analysis) is complex, expensive, and challenging. To address this issue, herein, we describe an integrated sample-in-digital-answer-out (SIDAO) diagnostic system incorporating DNA extraction and digital recombinase polymerase amplification, which enables rapid and quantitative nucleic acid analysis from bodily fluids within a disposable cartridge. Inside the cartridge, reagents are pre-stored in sterilized tubes, with an automated pipetting module allowing facile liquid transfer. For digital analysis, we fabricate a simple, single-layer polydimethylsiloxane microfluidic device and develop a novel and simple sample compartmentalization strategy. Sample solution is partitioned into an array of 40,044 fL-volume microwells by sealing the microfluidic device through the application of mechanical pressure. The entire analysis is performed in a portable, fully automated instrument. We evaluate the quantitative capabilities of the system by analyzing *Mycobacterium tuberculosis* genomic DNA from both spiked saliva and serum samples, and demonstrate excellent analytical accuracy and specificity. This SIDAO system provides a promising diagnostic platform for quantitative nucleic acid testing at the point-of-care.

Keywords Sample-in-answer-out · Microfluidics · Quantitation · Digital RPA · Molecular diagnostics · Tuberculosis

Introduction

Infectious diseases continue to pose a severe threat to global public health [1]. Accordingly, the rapid and accurate diagnosis of such disease states is critical in controlling and minimizing pathogen-associated injuries and deaths [2]. Nucleic acid testing (NAT) as a diagnostic tool is attractive, due to its intrinsically high specificity and sensitivity [3].

ABC Highlights: authored by *Rising Stars and Top Experts.*

Electronic supplementary material The online version of this article (https://doi.org/10.1007/s00216-018-1335-9) contains supplementary material, which is available to authorized users.

✉ Andrew J. deMello
andrew.demello@chem.ethz.ch

✉ Nongyue He
nyhe1958@163.com

[1] Institute for Chemical and Bioengineering, Department of Chemistry and Applied Biosciences, ETH Zürich, Vladimir-Prelog-Weg 1, 8093 Zürich, Switzerland

[2] Department of Biosystems Science and Engineering, ETH Zürich, 4058 Basel, Switzerland

[3] Economical Forest Cultivation and Utilization of 2011 Collaborative Innovation Center in Hunan Province, Hunan Key Laboratory of Biomedical Nanomaterials and Devices, Hunan University of Technology, Zhuzhou 412007, Hunan, China

[4] State Key Laboratory of Bioelectronics, School of Biological Science and Medical Engineering, Southeast University, Nanjing 210096, Jiangsu, China

[5] Department of Clinical Laboratory, The Affiliated Drum Tower Hospital of Nanjing University Medical School, Nanjing 210008, Jiangsu, China

[6] Department of Bionano Technology, Hanyang University, Sa-1-dong 1271, Ansan 15588, South Korea

However, NAT assays performed within centralized laboratories almost always involve the use of sophisticated benchtop instrumentation and skilled staff to ensure robust operation and prevention of cross-contamination. Thus, although NAT tests are far more efficient than culture-based methods [4] and enzyme-linked immunosorbent assays (ELISAs) [5] in terms of speed, sensitivity, and information content, they are habitually constrained to operation within well-equipped analytical laboratories. Further, while a simple positive/negative diagnosis of an infectious disease does not necessarily require quantitation, accurate determination of viral or bacterial load is crucial for establishing severity of infection and optimal course of treatment, monitoring treatment efficacy, and distinguishing between active infection and carrier status. Overall, the application of rapid and quantitative NAT assays in infectious diseases is an area of critical need.

To address the aforementioned problems, a number of automated, sample-in-answer-out molecular diagnostic platforms (integrating of nucleic acid extraction, amplification, and detection) have emerged in recent times [6, 7]. Current commercially available systems typically employ polymerase chain reaction (PCR)-based analytical methods (Table 1). Although NAT in such sample-in-answer-out systems can be performed in a highly efficiency manner, several critical shortcomings remain. For example, some of these systems still require certain off-device reagent manipulation (nos. 1, 3, 4, 6, 8, and 9 in Table 1), involving potential risk of cross-contamination. Others have large footprints (nos. 7, 8, and 9 in Table 1), and are thus not suitable for point-of-care testing (POCT). In this regard, a few versatile diagnostic platforms using programmable microfluidics can be used for sample-in-answer-out NAT (nos. 10, 11, and 12 in Table 1). However, all of these have a common and important limitation: they are incapable of quantifying nucleic acids, since quantitation based on analog analytical methods requires a reference or standard and the generation of a standard curve. This is complex, expensive, and challenging to achieve in an automated system.

Digital PCR (dPCR) is a single molecule counting technique that enables simple, precise, highly sensitive, and absolute quantification of nucleic acids without the need for a calibration curve [8, 9]. Accordingly, dPCR is of potential utility in the detection of pathogenic infections [10, 11], circulating biomarkers [12–14], genetic mutations [15, 16], DNA methylation [17, 18], drug resistance [19, 20], environmental microbes [21, 22], and genetically modified organisms [23, 24]. Inspired by these advances, isothermal recombinase polymerase amplification (RPA) [25, 26] has also been successfully transferred to digital format, namely dRPA [27–29]. This method is an attractive alternative to dPCR as it works at constant low temperatures (normally 37–42 °C), without the need for thermocycling. This means that consumables do not need to endure high temperatures and thus the challenges associated with system engineering are significantly reduced. Further, it is fast (with amplification times of ca. 20 min) and can be initiated with stable, lyophilized pellets [26]. Accordingly, the use of dRPA in point-of-care NAT should enable the development of a rapid, cost-effective, quantitative sample-in-answer-out diagnostic systems.

In digital amplification experiments, the assay sample must be separated into many (typically tens of thousands) isolated reaction vessels. Microfluidic devices provide an excellent

Table 1 Commercially available sample-in-answer-out molecular diagnostic systems

No.	System	Manufacturer (website)	Analytical method	Disposable container	Samples/run	Time to result (min)
1	GeneXpert®	Cepheid, USA (www.cepheid.com/us)	Real-time PCR	Cartridge	1–80	30–150
2	GenePOC™	GenePOC, Canada (www.genepoc-diagnostics.com)	Real-time PCR	Cartridge	1–8	70
3	ARIES®	Luminex, USA (www.luminexcorp.com)	Real-time PCR	Cassette	1–12	< 120
4	Integrated Cycler & Simplexa™	Focus Diagnostics, USA (www.focusdx.com)	Real-time PCR	Disc	1–8	60
5	FilmArray®	BioFire Diagnostics, USA (www.biofiredx.com)	Real-time PCR	Pouch	1	70
6	cobas® Liat®	Roche Diagnostics, USA (molecular.roche.com)	Real-time PCR	Tube segments	1	20
7	iCubate®	iCubate, USA (icubate.com)	PCR and microarray	Cassette	1–4	180–240
8	Unyvero™	Curetis, Germany (www.unyvero.com)	PCR and microarray	Cartridge	1–2	240–300
9	Rheonix CARD®	Rheonix, USA (rheonix.com)	PCR and microarray	Cartridge	1–24	360
10	Vivalytic	Bosch Healthcare Solutions, Germany (www.bosch-healthcare.com)	Real-time PCR and microarray	Cartridge	1	> 30
11	io®	Atlas Genetics, UK (www.atlasgenetics.com)	PCR and electrochemical sensor	Cartridge	1	30
12	ePlex®	GeneMark Dx, USA (www.genmarkdx.com)	PCR and electrochemical sensor	Cartridge	1–24	90

platform for achieving such a process [30, 31], through the generation of water-in-oil droplets [32–34], or isolation within physical microchambers [35–38]. Although both approaches have proven successful in research-based [30, 31] and commercial dPCR platforms [39, 40], the use of an oil phase, pneumatic/hydraulic valves, and/or complex multilayer microfluidic architectures poses significant challenges in regard to system engineering and cost-management. Accordingly, we sought to develop a simple compartmentalization mechanism that could be readily integrated in an automated workflow with minimal extraneous control. Herein, we report a novel sample compartmentalization strategy using a simple, single-layer polydimethylsiloxane (PDMS) microfluidic device, for dRPA assays. The sample solution is partitioned into 40,044 microwells by sealing the elastomeric microfluidic device through the application of mechanical pressure. By virtue of its simplicity, we were able to integrate this pressure-sealed microfluidic device into a previously developed qualitative nucleic acid testing system [41], to realize a novel and quantitative sample-in-digital-answer-out (SIDAO) system. As a proof-of-principle, *Mycobacterium tuberculosis* (MTB)-spiked serum and saliva samples were analyzed to evaluate the performance of the SIDAO system. Combining the advantages of simplicity, portability, rapidity (ca. 70 min), low-cost, and quantitative readout, we anticipate that the SIDAO system has great promise for accurate molecular diagnostic tests at the point-of-care.

Materials and methods

Materials and reagents

Magnetic beads (MBs), lysis buffer, binding buffer, wash buffers I and II, and elution buffer were made according to published protocols [42, 43]. The TwistAmp® exo kit was purchased from TwistDx Ltd. (Cambridge, UK). The oligonucleotide primers and exonuclease probe (see Electronic Supplementary Material (ESM) Table S1) were synthesized by Sangon Biotech Ltd. (Shanghai, China) and the H37Rv *M. tuberculosis* strain and saliva and serum samples were acquired from Nanjing Drum Tower Hospital.

Microfluidic chip design and fabrication

The microfluidic device was fabricated using conventional multilayer soft lithography. Briefly, high-resolution film and chrome photomasks were fabricated using two separate designs for the microchannel and microwell patterns, respectively. Patterns were designed using AutoCAD 2016 (Autodesk GmbH, Munich, Germany). A two-level master was prepared on a silicon wafer using a multilayer SU-8 photoresist (MicroChem, Westborough, USA) with the aid of a mask aligner (UV-KUB 3, Kloé Ltd., Montpellier, France) and then exposed to trichloro(1H,1H,2H,2H-perfluorooctyl)silane (Sigma-Aldrich, Buchs, Switzerland) for 2 h. A single device contained 40,044 cylindrical microwells, each with a diameter and depth of 5.0 μm (defining a volume of 98 fL). Sylgard 184 PDMS base and curing agent (Dow Corning, Midland, USA) were mixed at a ratio of 10:1 wt/wt, degassed, and decanted onto the master. The entire structure was then oven-cured at 70 °C for 2 h. After curing, inlet and outlet ports were punched through the structured PDMS layer, with subsequent bonding to a flat PDMS substrate by plasma treatment and incubation on a hot plate at 95 °C for at least 2 h.

Cartridge design

The cartridge (14 cm long, 3 cm wide, 13 cm high) comprised a housing, a pipettor, a sliding vane module, a set of sample tubes

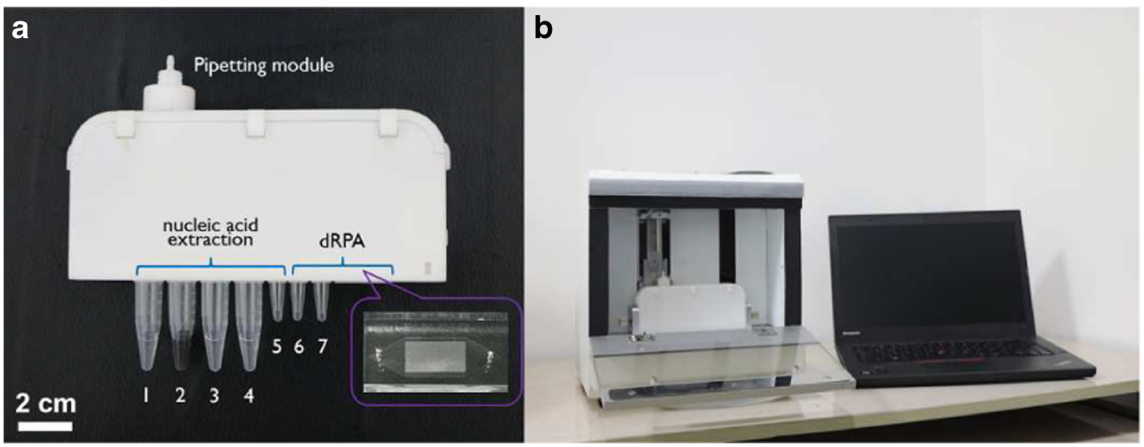

Fig. 1 (**A**) The SIDAO cartridge containing sample tubes pre-loaded with assay reagents. The reagents, as labeled in the picture, are (1) lysis buffer, (2) magnetic beads within a binding buffer, (3) wash buffer I, (4) wash buffer II, (5) elution buffer, (6) RPA mix, and (7) magnesium acetate solution. (**B**) The entire SIDAO instrument positioned beside a notebook PC

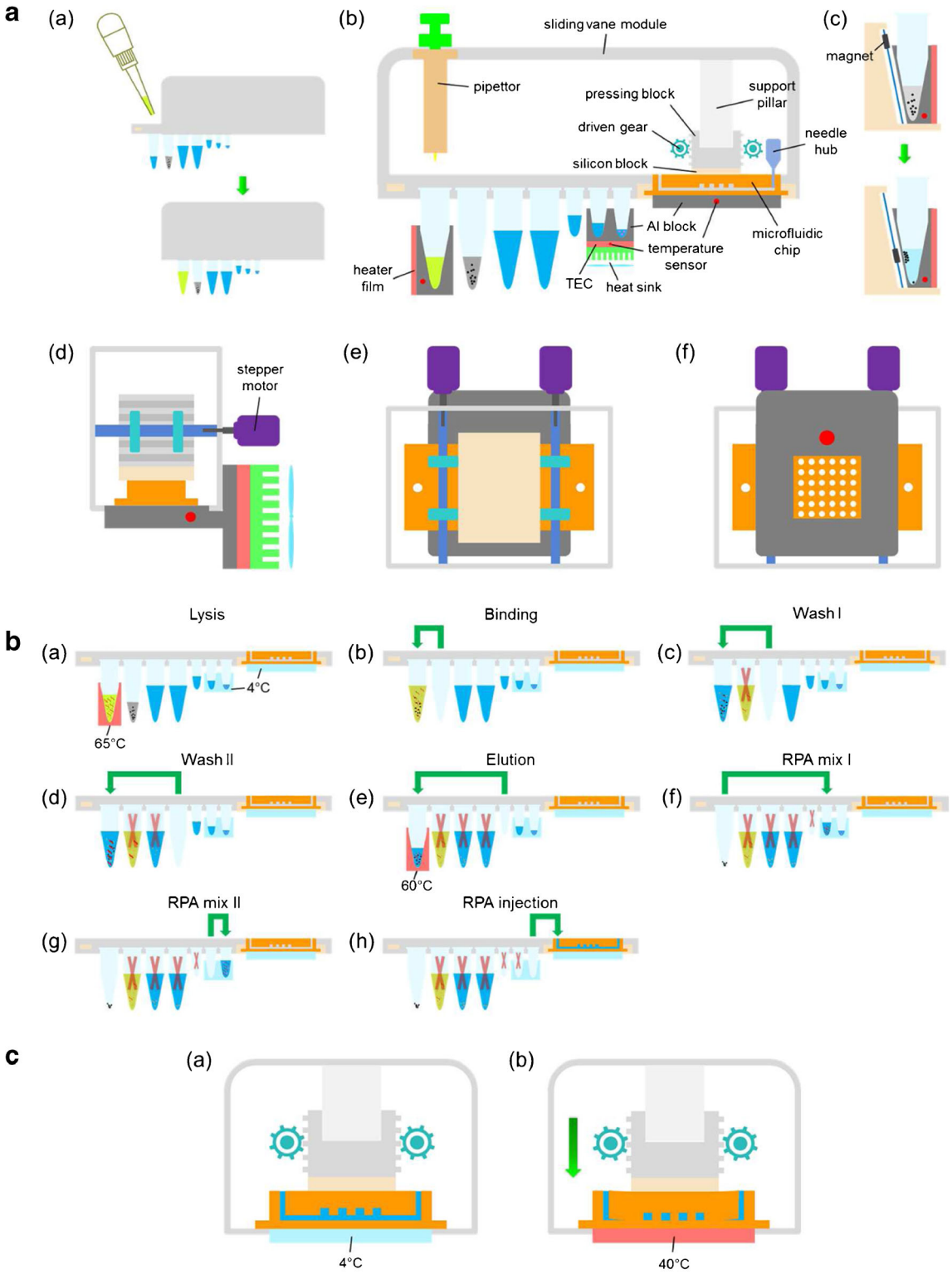

Fig. 2 Schematics of the sample preparation process and the dRPA assay. (**A**) Profile of the cartridge containing functional modules, showing (**a**) sample loading and (**b**–**f**) structures for the pipetting, heating/cooling, and pressing modules. (**c**) shows the magnetic separation function. Modules within and outside the cartridge are shown from the (**b**) front, (**d**) side, (**e**) top, and (**f**) bottom. (**B**) Automated pipetting steps showing (**a**–**e**) nucleic acid extraction and (**f**–**h**) RPA preparation. (**C**) The pressure-sealing procedure for compartmentalization of the RPA reaction solution, (**a**) before and (**b**) during the assay

with pre-stored reagents, a microfluidic device, and a pressure-sealing module (Figs. 1A and 2A(b)). All components were produced by 3D printing a polycarbonate resin using a RAISE 3D N2 Plus printer (Raise3D, Costa Mesa, USA) and manually assembled with several simple parts (i.e., a spring, plastic vane, elastomeric sheet, and centrifuge tube).

Instrument design

The portable instrument measured 27 × 28 × 25 cm and weighed 6.5 kg (Fig. 1B). The pipetting force was provided by a plunger pump (MP250-2L-A1C2000, Longer Precision Pump Ltd., Baoding, China). The heating/cooling modules for the RPA assay were built using two Peltier devices, each consisting of a thermoelectric cooler (TEC1-127xx3030, KJLP Electronics, Shenzhen, China), a temperature sensor (PT100 B sensor, Heraeus, Hanau, Germany), and a heat sink. Pipettor and magnet (used to perform magnetic separation) motions were achieved using two stepper motors (42SH47-2A, Changzhou Fulling Motor Ltd., Changzhou, China) and one micro stepper motor with slider (Tmall Marketplace Ltd., Hangzhou, China), respectively. Microfluidic device sealing was performed using a square block, driven by two small stepper motors (28SH45-0956A, Changzhou Fulling Motor Ltd., Changzhou, China) with pinions. Fluorescence images were obtained using a custom optical module, incorporating a charge coupled device (CCD) camera (E3ISPM, ToupTek Photonics Ltd., Hangzhou, China).

Reagent pre-storage

Nucleic acid extraction was performed using a previously defined protocol [42–44]. Specifically, 400 μL of lysis buffer, 50 μL of binding buffer with 0.5 mg of MBs, 500 μL of wash buffer I, 500 μL of wash buffer II, and 200 μL of elution buffer were used. The dRPA assay was executed with 34.3 μL of RPA Mix and 2.5 μL of 280 mM magnesium acetate. The RPA Mix was prepared by dissolving lyophilized RPA proteins with 2.1 μL of 10 μM oligonucleotide primers, 0.6 μL of 10 μM exonuclease probe, 0.5 μL of 0.2% Tween-20, 2.8 μL of sterile water, and 29.5 μL of rehydration buffer (from the TwistAmp® exo kit). All reagents were pre-loaded into sterilized centrifuge tubes and sealed with adhesive foils within the disposable cartridge.

Nucleic acid extraction and dRPA assay

MTB gDNA was extracted using a previously defined protocol [42–44]. In brief, 100 μL of sample was added to a lysis buffer and incubated at room temperature for 5 min. The mixture was transferred to the binding buffer containing MBs and incubated for 3 min. The supernatant was discarded after magnetic separation for 30 s by applying an external magnetic field. Subsequently, magnetic complexes were rinsed with wash buffers I and II to remove excess reagents. The elution buffer was then added to the magnetic complexes and incubated at 65 °C for 10 min. Finally, the purified DNA was collected for the subsequent dRPA assay.

Digital RPA was performed according to the manufacturer's protocol, with minor modification. Briefly, 10 μL of DNA template was added to the RPA Mix. Magnesium acetate was then added to the mixture to a final concentration of 25 mM at 4 °C. The final reaction mixture was transferred and injected into the microfluidic device. After all microchambers had been filled with reaction mixture, the chip was sealed to form 40,044 isolated microreactors. The RPA reaction was immediately carried out at 39 °C for 20 min.

Data acquisition and analysis

Fluorescence images were obtained using the custom optical module mounted within the instrument. The stock concentration of MTB gDNA (c_0) in the dRPA chip was calculated according to Eq. 1 [36, 45],

$$c_0 = -ln(1-f_0)/V_0 \quad (1)$$

Here, f_0 is the fraction of positive microwells and V_0 is the volume of one microwell. Subsequently, the concentration of extracted MTB gDNA (c) was calculated using Eq. 2, i.e.,

$$c = c_0/d = -ln(1-f_0)/dV_0 \quad (2)$$

where d is the dilution factor. In the current experiments, d = 10.5 μL/50 μL = 0.21.

Results and discussion

Device operation

As noted, the system used in the current studies consists of two components: a cartridge (housing reagents, the pipettor, microfluidic device, and square block) and a portable instrument (that processes the cartridge and houses the liquid handling, heating/cooling, magnetic separation, and optical systems). The cartridge (Fig. 1A) has a number of useful features. First, it is enclosed to prevent pathogen exposure and cross-contamination. Second, reagents may be pre-stored and sealed for extended periods of time. Finally, the cartridge incorporates 3D printed components (the housing, pipettor, square block), which ensures rapid and cost-effective fabrication.

Prior to operation, the nucleic acid extraction and RPA reagents were delivered to the appropriate sample tube, sealed with adhesive foil, and loaded into the cartridge. Sample is

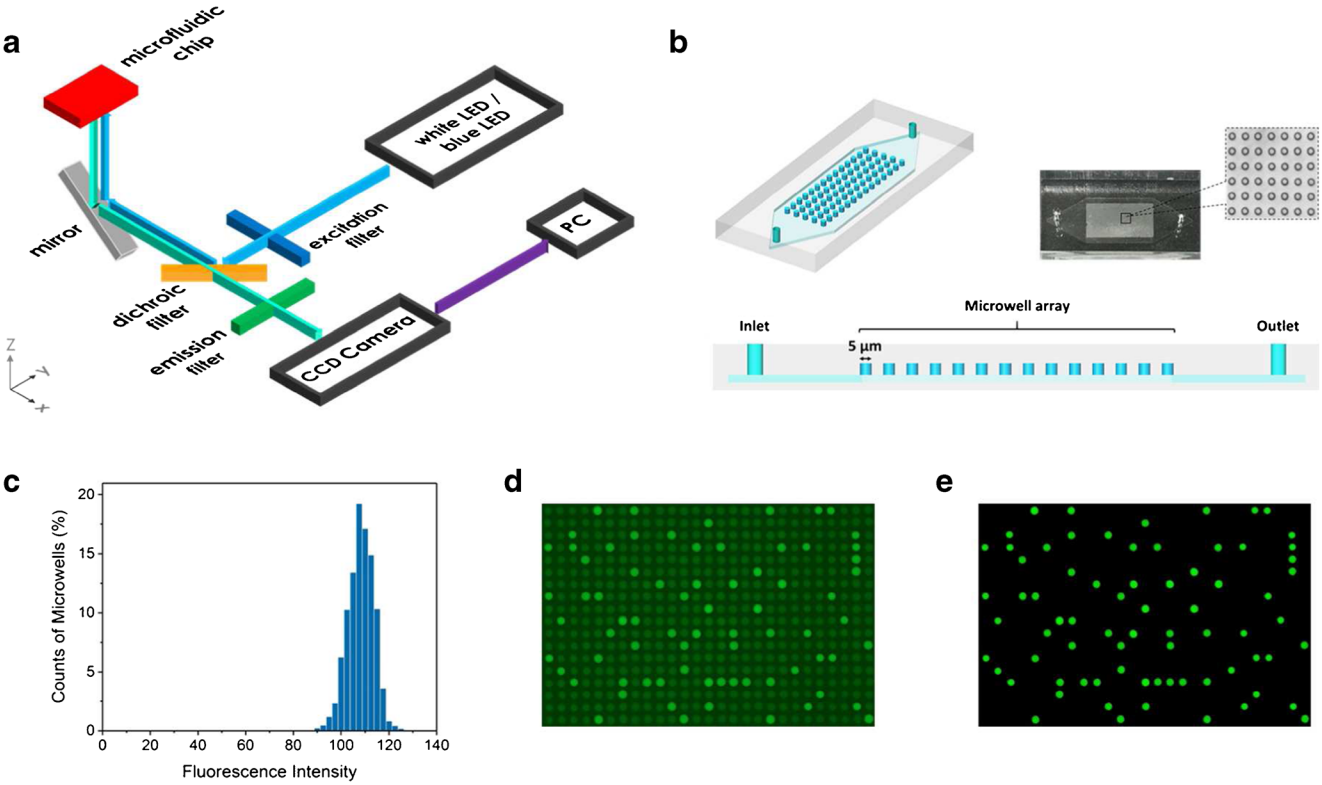

Fig. 3 (**A**) Schematic of the optical system used for microwell array imaging. (**B**) Schematic and photograph of the microfluidic device. The volume of each microwell is 98.1 ± 0.8 fL. (**C**) A histogram of the integrated intensity from each microwell within the array. (**D**) Raw image of the chip after assay completion. (**E**) Modified image after contrast enhancement

then simply added to the first tube, and the entire cartridge loaded into the instrument. All proceeding steps are automated. Fluid transfer and mixing is performed by the pipettor (in the cartridge), and the plunge pump and two stepper motors (outside the cartridge). The plunge pump generates the pipetting force, with the stepper motors controlling horizontal and vertical motion. Magnetic bead separation was performed by moving a permanent magnet close to the exterior wall of the sample tube, using a micro stepper motor with slider (Fig. 2A (c)). The heating module for nucleic acid extraction uses a heater film attached to the aluminum block holding the sample tube (Fig. 2A(b, c)). The microfluidic device is housed adjacent to the sample tubes and located under a square block in the cartridge. The square block comprises a polymer slab adhered to an elastomeric sheet, providing a cushion to prevent microwell collapse when pressure-sealing is executed. The vertical motion of the square block is controlled using two stepper motors adjacent to the cartridge (Fig. 2A(d, e), ESM Note S1). Pressure-sealing allows sample compartmentalization within the microwell array in a simple manner and obviates the need for an oil phase, pneumatic/hydraulic valves, and complex microfluidic multilayer architectures. Additionally, two Peltier devices were used to keep the RPA reagents at 4 °C prior to use and to heat reagents to 40 °C during the assay (Fig. 2A(b, d)). A T-shaped aluminum block assists heat transfer from the Peltier to the microfluidic device (Fig. 2A(d)).

The workflow associated with the SIDAO analysis is illustrated in Fig. 2B. The sample is loaded into the first sample tube (containing lysis buffer) and the cartridge inserted into the instrument. The sample is lysed, releasing MTB gDNA. The MBs in binding buffer (tube 2) are transferred into the sample tube to capture gDNA. The magnet then moves into position and immobilizes MB/gDNA complexes. Washing is performed by discarding the first supernatant, and then rinsing with wash buffers I (tube 3) and II (tube 4). The purified gDNA is eluted using the buffer from tube 5, and transferred into tube 6 to mix with the RPA reagents. Next, the sample is added to a magnesium acetate solution (tube 7) and immediately injected into the microfluidic device. The reaction solution is compartmentalized into a large number of microwells by pressure-sealing the array (Fig. 2C). Finally, a fluorescence image of the entire array is recorded and subsequently analyzed.

Optimization of automated nucleic acid extraction

The accuracy and precision associated with pipetting were assessed using a Pipette Accuracy Tester (AD-4212B-PT, A&D Ltd., Tokyo, Japan) by dispensing four different volumes of water. As shown in ESM Table S2, results indicate superior accuracy and precision of the current pipettor than demanded by ISO 8655 Pipetting Standards [46]. Automated MTB gDNA extraction was then

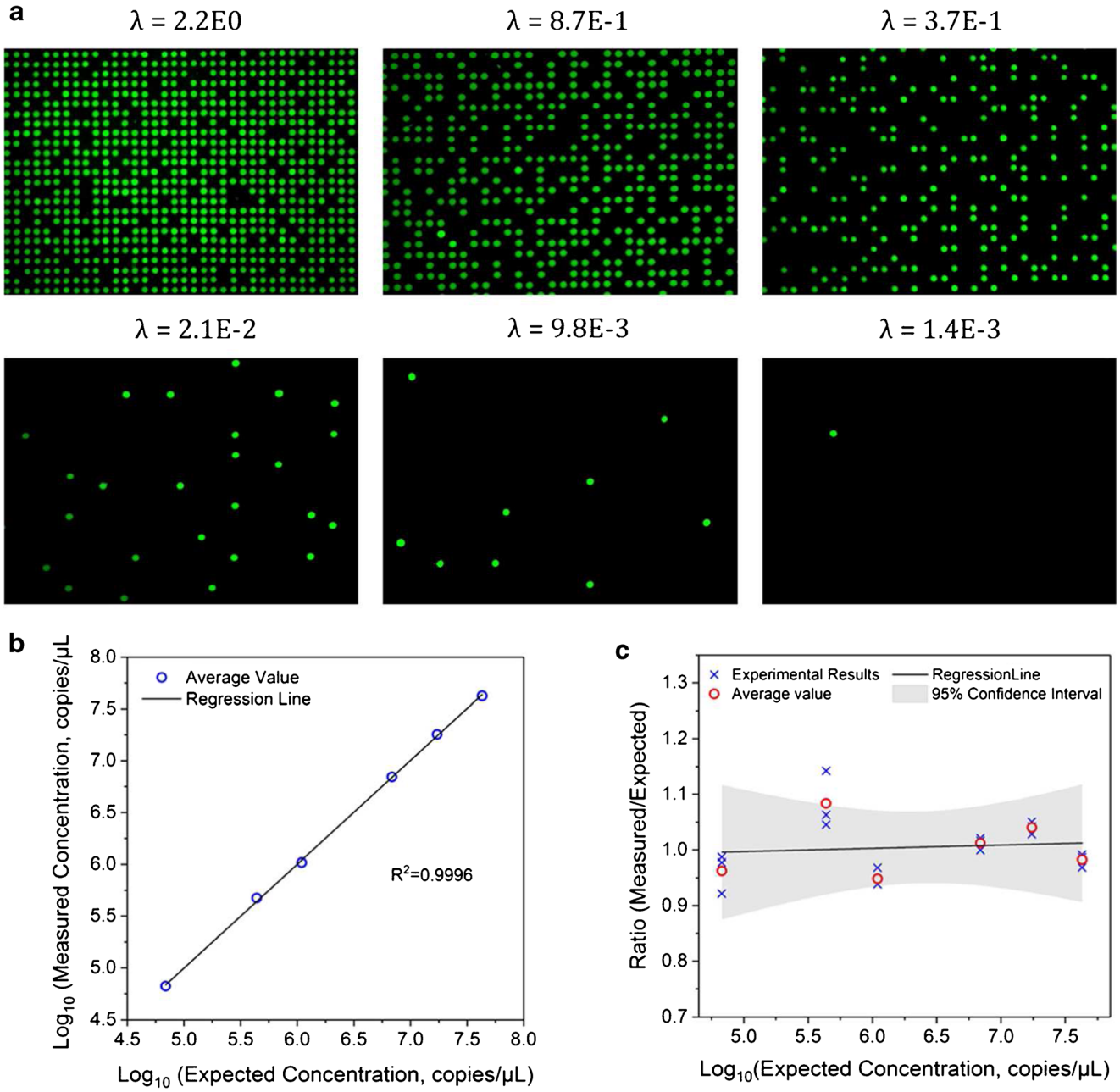

Fig. 4 Digital RPA analysis using the SIDAO system. (**A**) Digital RPA fluorescence images of MTB, with serial dilutions of target gDNA ranging from 6.9×10^4 to 1.1×10^8 copies/μL. λ represents the average number of copies per microwell. (**B**) Correlation between measured and the expected concentrations of MTB gDNA. (**C**) Comparison of the ratios of the measured/expected concentration to the expected concentration of MTB gDNA

performed. The extracted MTB gDNA was identified via agarose gel analysis. Clearly visible bands in all replicates indicated successful DNA extraction (ESM Fig. S1). To enhance DNA capture efficiencies, suspension mixing was added to the binding step to prevent MB settling. Subsequently, the pipettor was programmed to "draw in" and "push out" suspension under six different instructions, i.e., null (no operation) and suspension mixing at 0.1, 0.2, 0.5, 1.0, and 2.0 Hz. Results indicated that the MTB gDNA yield increased as a function of mixing frequency (ESM Fig. S2), noting that use of a mixing frequency above 2.0 Hz led to the formation of bubbles and resulted in reaction failure. A mixing rate of 1.0 Hz was found to be optimal in the current experiments.

Microwell array formation by pressure-sealing

A pressure-sealing module was used to compartmentalize the RPA reaction mixture, as shown in Fig. 2C. The mixture was automatically loaded into the dRPA device with

the pipettor, and forced into the microwells under pressure. Excess liquid was collected from the outlet into the needle hub (Fig. 2A(b)). With the pressure applied to its top surface, the elastomeric PDMS device deformed to efficiently seal all microwells. To confirm the efficacy of the pressure-sealing procedure, a photobleaching test was performed using an aqueous solution of fluorescein [35]. Briefly, a vertical line of microwells was exposed to a 60-mW beam at 488 nm for a period of 1 min. Subsequently, emission across the array was monitored (using low-intensity exposure). Results show that significant photobleaching was observed after laser exposure, with no fluorescence recovery seen at later times (ESM Fig. S3). These data strongly suggest that individual microwells are well-sealed and prevent exchange of dye between compartments.

Fluorescence analysis

A schematic in Fig. 3A shows the optical path of the custom optical module. Components were arranged so as to minimize the overall instrumental footprint. A blue LED source (475 nm) was used to excite green emission (525 nm) within microwells, with images being captured using an auto-focused CCD camera. Figure 3B shows the geometry of the microchamber array and highlights facile compartmentalization of dRPA reagents by pressure-sealing. To test the uniformity of the microfluidic device, an aqueous fluorescein solution was delivered to all 44,044 microwells, with the fluorescence intensities from each microwell being measured [45]. As shown in Fig. 3C, data revealed that intensities range between 100 and 115 (arbitrary units) with a coefficient of variation (CV) of 4.9%, indicating solution partitioning is a highly uniform process.

To assess the feasibility of digital quantitation, dRPA with positive control templates was performed in the microfluidic device. Figure 3D shows a raw image obtained after a 30-min reaction. It can be seen that positive microwells (i.e., those containing target DNA) exhibited significantly stronger emission than empty microwells, indicating a successful dRPA assay. To automate the counting of positive microwells, the raw image was further modified by contrast enhancement to remove background (Fig. 3E). A K-means clustering algorithm was used for fluorescence dot counting in the modified image.

Absolute quantification of MTB gDNA by dRPA

To test the performance of the SIDAO system as a NAT diagnostic, six sets of experiments were performed using a serial dilution of a MTB gDNA stock solution of known concentration. The gDNA was extracted from the H37Rv MTB strain (with high-level colony-forming units) within the cartridge, followed by measurement of its mass concentration (520.75 ng/μL) as a reference. The stock gDNA was serially diluted and copy number concentrations calculated using a spectrophotometer ("expected" result) and our SIDAO system ("measured" result) (ESM Tables S3, S4). Figure 4A shows representative fluorescence images from these experiments. It can be seen that the fraction of positive microwells decreases proportionally with gDNA dilution. Positive microwells (showing green emission) were distributed randomly in each experiment, confirming Poisson statistics. Furthermore, and as shown in Fig. 4B, the logarithm of the measured gDNA concentration exhibited a linear correlation with the logarithm of the expected value ($R^2 = 0.9996$), demonstrating the accuracy of the SIDAO system for MTB gDNA quantitation. A plot of the ratio of measured/expected concentrations against the logarithm of the expected value is also shown Fig. 4C. It can be seen that 17 of 18 experimental tests were within the 95% confidence interval, with all tests falling within the 99% confidence interval. Accordingly, the initial concentration of MTB gDNA can be detected with our SIDAO system in a precise and rapid manner.

To further evaluate system performance, we compared MTB quantification using three different sample-to-answer strategies, i.e., (a) the automated SIDAO assay, (b) a manual SIDAO assay, and (c) an integrated but manual DNA extraction and qPCR assay. Inspection of Fig. 5 confirms that consistent results were obtained using all methods. The measured average stock concentration of MTB gDNA was 4.25×10^5 (a), 4.54×10^5 (b), and 3.94×10^5 (c) copies/μL. Significantly, we note that the smallest standard deviation was achieved using the automated SIDAO assay.

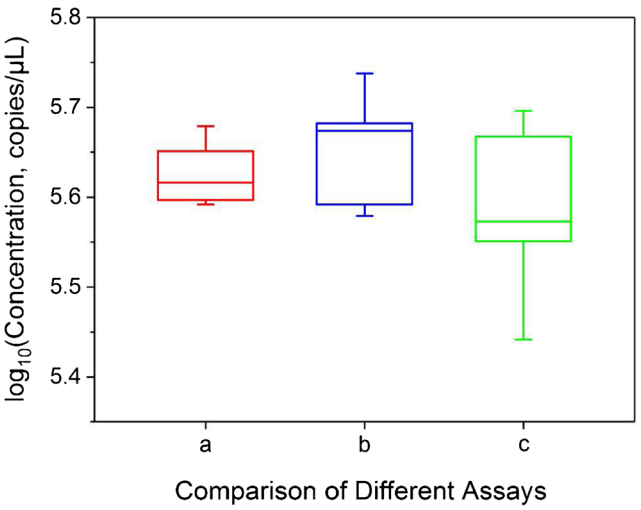

Fig. 5 Comparison of MTB gDNA copy number quantification assays. (**a**) The automated SIDAO assay. (**b**) A manual SIDAO assay. (**c**) An integrated but manual DNA extraction and qPCR assay

Table 2 Recovery and specificity tests for MTB (2.89×10^8 CFU)

Sample	Measured MTB gDNA (copies/extraction)	Recovery rate of MTB gDNA (%)
MTB	1.70×10^7	N/A
MTB spiked saliva	1.55×10^7	91.3
MTB spiked serum	1.39×10^7	81.7
MM[a]	1.63×10^7	N/A
MM spiked saliva	1.46×10^7	89.4
MM spiked serum	1.30×10^7	79.6
MNTM[b]	N[c]	N/A
MNTM spiked saliva	N	N/A
MNTM spiked serum	N	N/A

[a] Mixed mycobacteria (MM) consists of MTB, *M. abscessus*, and *M. chelonae*

[b] Mixed non-tuberculous mycobacteria (MNTM) consists of *M. abscessus* and *M. chelonae*

[c] Negative

Recovery and specificity tests

To assess performance of the SIDAO system in the analysis of real-world samples, recovery and specificity tests were carried out using 2.9×10^8 CFU of MTB, mixed mycobacteria (MM), and mixed non-tuberculous mycobacteria (MNTM) cells, spiked in serum and saliva samples, respectively. As shown in Table 2, we found that the recovery rate of MTB gDNA was 91.3% in spiked saliva and 81.7% in spiked serum. MTB gDNA was also quantitatively detected in MM spiked saliva and serum with a recovery rate of 89.4 and 79.6%, respectively. It should be noted that significantly higher recovery was achieved when using saliva rather than serum. This may be caused by difficulties in lysing the MTB in serum, since it has a more complex biomolecular composition. On the contrary, MTB gDNA was not detected from MNTM spiked saliva/serum, delivering negative results. Put simply, these results indicate that the detection of MTB with our system is highly specific, with recovery occurring at an acceptable level.

Conclusions

Herein, we have presented a novel NAT system that integrates sample preparation and digital analysis within a disposable cartridge, for rapid and quantitative detection of MTB directly from clinical samples. The system integrates a simple pressure-sealed microfluidic chip for sample compartmentalization and digital analysis. Significantly, the sealing mechanism does not require complex control systems (e.g., pneumatics, hydraulics, or valves), needing only a simple mechanical press to function. To the best of our knowledge, this is the first demonstration of such a mechanism in digital nucleic acid analyses. Furthermore, we have explored the integration of nucleic acid extraction and detection, in an effort to provide a quantitative sample-in-answer-out methodology. Combining extraction and detection is a key feature of the current system, since most nucleic acid targets cannot be directly detected from untreated biological samples. As digital quantification is based on simple end-point counting, quantitation is readily performed without the need for complex standard curve analysis. We have verified the accuracy of the SIDAO system for quantitative detection of MTB gDNA by comparison with a MTB gDNA standard, and have demonstrated high recovery rates (ca. 90% in saliva, ca. 80% in serum), indicating the efficacy of our system for real-world sample analysis. Since the 3D printed polymer cartridge is disposable, inexpensive, and runs in a portable, fully automated instrument, we envision that the SIDAO system will be used as a POCT for infectious disease diagnosis.

Acknowledgments This work was supported by the Swiss Federal Institute of Technology (ETH Zürich), the National Research Foundation of Korea (Grant Nos. 2008-0061891 and 2009-00426), the National Natural Science Foundation of China (Grant No. 61527806), the Hunan Key Research Project (Grant No. 2017SK2174), and the China Postdoctoral Science Foundation (Grant No. 2018M630498). P.D.H. acknowledges support from European Union's Horizon 2020 research and innovation program through the Individual Marie Skłodowska-Curie Fellowship "Ampidots" under grant agreement no. 701994.

Compliance with ethical standards

The studies described herein were approved by Nanjing Drum Tower Hospital Clinical Research Ethics Committee, and have been performed in accordance with ethical standards. Informed consent was obtained from all participants.

Conflict of interest The authors declare that they have no conflict of interest.

References

1. Fauci AS, Morens DM. The perpetual challenge of infectious diseases. N Engl J Med. 2012;366(5):454–61. https://doi.org/10.1056/NEJMra1108296.
2. Holmes KK, Bertozzi S, Bloom BR, Jha P. Disease control priorities, third edition: volume 6. Major infectious diseases. World Bank Publications; 2017.
3. Hans R, Marwaha N. Nucleic acid testing-benefits and constraints. Asian J Transfus Sci. 2014;8(1):2–3. https://doi.org/10.4103/0973-6247.126679.
4. Asmar S, Drancourt M. Rapid culture-based diagnosis of pulmonary tuberculosis in developed and developing countries. Front Microbiol. 2015;6:1184. https://doi.org/10.3389/fmicb.2015.01184.
5. Lequin RM. Enzyme immunoassay (EIA)/enzyme-linked immunosorbent assay (ELISA). Clin Chem. 2005;51(12):2415–8. https://doi.org/10.1373/clinchem.2005.051532.
6. Danielson PB, McKiernan HE, Legg KM. Chapter 5—Integrated polymerase chain reaction technologies (sample-to-answer technologies). In: Molecular diagnostics. 3rd ed. Elsevier; 2017. p. 59–78. https://doi.org/10.1016/B978-0-12-802971-8.00005-5.

7. Perkins MD, Kessel M. What Ebola tells us about outbreak diagnostic readiness. Nat Biotechnol. 2015;33(5):464–9. https://doi.org/10.1038/nbt.3215.
8. Vynck M, Vandesompele J, Thas O. Quality control of digital PCR assays and platforms. Anal Bioanal Chem. 2017;409(25):5919–31. https://doi.org/10.1007/s00216-017-0538-9.
9. Duewer DL, Kline MC, Romsos EL, Toman B. Evaluating droplet digital PCR for the quantification of human genomic DNA: converting copies per nanoliter to nanograms nuclear DNA per microliter. Anal Bioanal Chem. 2018;410(12):2879–87. https://doi.org/10.1007/s00216-018-0982-1.
10. Bruner KM, Murray AJ, Pollack RA, Soliman MG, Laskey SB, Capoferri AA, et al. Defective proviruses rapidly accumulate during acute HIV-1 infection. Nat Med. 2016;22(9):1043–9. https://doi.org/10.1038/nm.4156.
11. Pavsic J, Devonshire A, Blejec A, Foy CA, Van Heuverswyn F, Jones GM, et al. Inter-laboratory assessment of different digital PCR platforms for quantification of human cytomegalovirus DNA. Anal Bioanal Chem. 2017;409(10):2601–14. https://doi.org/10.1007/s00216-017-0206-0.
12. Zou Z, Qi P, Qing ZH, Zheng J, Yang S, Chen WJ, et al. Technologies for analysis of circulating tumour DNA: progress and promise. TrAC Trends Anal Chem. 2017;97:36–49. https://doi.org/10.1016/j.trac.2017.08.004.
13. Gorgannezhad L, Umer M, Islam MN, Nguyen NT, Shiddiky MJA. Circulating tumor DNA and liquid biopsy: opportunities, challenges, and recent advances in detection technologies. Lab Chip. 2018;18(8):1174–96. https://doi.org/10.1039/c8lc00100f.
14. Ye W, Tang XJ, Liu C, Wen CW, Li W, Lyu JX. Accurate quantitation of circulating cell-free mitochondrial DNA in plasma by droplet digital PCR. Anal Bioanal Chem. 2017;409(10):2727–35. https://doi.org/10.1007/s00216-017-0217-x.
15. Kakiuchi M, Nishizawa T, Ueda H, Gotoh K, Tanaka A, Hayashi A, et al. Recurrent gain-of-function mutations of RHOA in diffuse-type gastric carcinoma. Nat Genet. 2014;46(6):583–7. https://doi.org/10.1038/ng.2984.
16. Whale AS, Devonshire AS, Karlin-Neumann G, Regan J, Javier L, Cowen S, et al. International interlaboratory digital PCR study demonstrating high reproducibility for the measurement of a rare sequence variant. Anal Chem. 2017;89(3):1724–33. https://doi.org/10.1021/acs.analchem.6b03980.
17. Wu Z, Bai Y, Cheng Z, Liu F, Wang P, Yang D, et al. Absolute quantification of DNA methylation using microfluidic chip-based digital PCR. Biosens Bioelectron. 2017;96:339–44. https://doi.org/10.1016/j.bios.2017.05.021.
18. Pharo HD, Andresen K, Berg KCG, Lothe RA, Jeanmougin M, Lind GE. A robust internal control for high-precision DNA methylation analyses by droplet digital PCR. Clin Epigenetics. 2018;10 https://doi.org/10.1186/s13148-018-0456-5.
19. Murtaza M, Dawson SJ, Tsui DW, Gale D, Forshew T, Piskorz AM, et al. Non-invasive analysis of acquired resistance to cancer therapy by sequencing of plasma DNA. Nature. 2013;497(7447):108–12. https://doi.org/10.1038/nature12065.
20. Hata AN, Niederst MJ, Archibald HL, Gomez-Caraballo M, Siddiqui FM, Mulvey HE, et al. Tumor cells can follow distinct evolutionary paths to become resistant to epidermal growth factor receptor inhibition. Nat Med. 2016;22(3):262–9. https://doi.org/10.1038/nm.4040.
21. Tadmor AD, Ottesen EA, Leadbetter JR, Phillips R. Probing individual environmental bacteria for viruses by using microfluidic digital PCR. Science. 2011;333(6038):58–62. https://doi.org/10.1126/science.1200758.
22. Mehle N, Dobnik D, Ravnikar M, Novak MP. Validated reverse transcription droplet digital PCR serves as a higher order method for absolute quantification of potato virus Y strains. Anal Bioanal Chem. 2018;410(16):3815–25. https://doi.org/10.1007/s00216-018-1053-3.
23. Niu CQ, Xu YC, Zhang C, Zhu PY, Huang KL, Luo YB, et al. Ultrasensitive single fluorescence-labeled probe-mediated single universal primer-multiplex-droplet digital polymerase chain reaction for high-throughput genetically modified organism screening. Anal Chem. 2018;90(9):5586–93. https://doi.org/10.1021/acs.analchem.7b03974.
24. Demeke T, Dobnik D. Critical assessment of digital PCR for the detection and quantification of genetically modified organisms. Anal Bioanal Chem. 2018;410(17):4039–50. https://doi.org/10.1007/s00216-018-1010-1.
25. Piepenburg O, Williams CH, Stemple DL, Armes NA. DNA detection using recombination proteins. PLoS Biol. 2006;4(7):1115–21. https://doi.org/10.1371/journal.pbio.0040204.
26. Stringer OW, Andrews JM, Greetham HL, Forrest MS. TwistAmp (R) Liquid: a versatile amplification method to replace PCR. Nat Methods. 2018;15(5):I–Iii.
27. Yeh EC, Fu CC, Hu L, Thakur R, Feng J, Lee LP. Self-powered integrated microfluidic point-of-care low-cost enabling (SIMPLE) chip. Sci Adv. 2017;3(3) https://doi.org/10.1126/sciadv.1501645.
28. Schuler F, Schwemmer F, Trotter M, Wadle S, Zengerle R, von Stetten F, et al. Centrifugal step emulsification applied for absolute quantification of nucleic acids by digital droplet RPA. Lab Chip. 2015;15(13):2759–66. https://doi.org/10.1039/c5lc00291e.
29. Li Z, Liu Y, Wei QQ, Liu YJ, Liu WW, Zhang XL, et al. Picoliter well array chip-based digital recombinase polymerase amplification for absolute quantification of nucleic acids. PLoS One. 2016;11(4) https://doi.org/10.1371/journal.pone.0153359.
30. Ven KR, Vanspauwen B, Perez-Ruiz E, Leirs K, Decrop D, Gerstmans H, et al. Target confinement in small reaction volumes using microfluidic technologies: a smart approach for single-entity detection and analysis. ACS Sensors. 2018;3(2):264–84. https://doi.org/10.1021/acssensors.7b00873.
31. Cao L, Cui XY, Hu J, Li ZD, Choi JR, Yang QZ, et al. Advances in digital polymerase chain reaction (dPCR) and its emerging biomedical applications. Biosens Bioelectron. 2017;90:459–74. https://doi.org/10.1016/j.bios.2016.09.082.
32. Zhang YH, Jiang HR. A review on continuous-flow microfluidic PCR in droplets: advances, challenges and future. Anal Chim Acta. 2016;914:7–16. https://doi.org/10.1016/j.aca.2016.02.006.
33. Zhu PA, Wang LQ. Passive and active droplet generation with microfluidics: a review. Lab Chip. 2017;17(1):34–75. https://doi.org/10.1039/c6lc01018k.
34. Kosir AB, Divieto C, Pavsic J, Pavarelli S, Dobnik D, Dreo T, et al. Droplet volume variability as a critical factor for accuracy of absolute quantification using droplet digital PCR. Anal Bioanal Chem. 2017;409(28):6689–97. https://doi.org/10.1007/s00216-017-0625-y.
35. Men YF, Fu YS, Chen ZT, Sims PA, Greenleaf WJ, Huang YY. Digital polymerase chain reaction in an array of femtoliter polydimethylsiloxane microreactors. Anal Chem. 2012;84(10):4262–6. https://doi.org/10.1021/ac300761n.
36. Heyries KA, Tropini C, VanInsberghe M, Doolin C, Petriv OI, Singhal A, et al. Megapixel digital PCR. Nat Methods. 2011;8(8):649–U64. https://doi.org/10.1038/nmeth.1640.
37. Low HY, Chan SJ, Soo GH, Ling B, Tan EL. Clarity (TM) digital PCR system: a novel platform for absolute quantification of nucleic acids. Anal Bioanal Chem. 2017;409(7):1869–75. https://doi.org/10.1007/s00216-016-0131-7.
38. Shen F, Sun B, Kreutz JE, Davydova EK, Du W, Reddy PL, et al. Multiplexed quantification of nucleic acids with large dynamic range using multivolume digital RT-PCR on a rotational SlipChip tested with HIV and hepatitis C viral load. J Am Chem Soc. 2011;133(44):17705–12. https://doi.org/10.1021/ja2060116.
39. Hindson CM, Chevillet JR, Briggs HA, Gallichotte EN, Ruf IK, Hindson BJ, et al. Absolute quantification by droplet digital PCR

versus analog real-time PCR. Nat Methods. 2013;10(10):1003–5. https://doi.org/10.1038/nmeth.2633.
40. Baker M. Digital PCR hits its stride. Nat Methods. 2012;9(6):541–4. https://doi.org/10.1038/nmeth.2027.
41. Chen H, Wu YQ, Chen Z, Hu ZL, Fang YL, Liao P, et al. Performance evaluation of a novel sample in-answer out (SIAO) system based on magnetic nanoparticles. J Biomed Nanotechnol. 2017;13(12):1619–30. https://doi.org/10.1166/jbn.2017.247.
42. Ali Z, Liang WB, Jin L, Tang YJ, Mou XB, Shah MAA, et al. Development of magnetic nanoparticles based nucleic acid extraction method and application in hepatitis C virus chemiluminescent detection. Sci Adv Mater. 2015;7(7):1233–40. https://doi.org/10.1166/sam.2015.1974.
43. Ali ZS, Wang JH, Mou XB, Tang YJ, Li TT, Liang WB, et al. Integration of nucleic acid extraction protocol with automated extractor for multiplex viral detection. J Nanosci Nanotechnol. 2017;17(2):862–70. https://doi.org/10.1166/jnn.2017.12613.
44. Wang JH, Ali ZS, Wang NY, Liang WB, Liu HN, Li F, et al. Simultaneous extraction of DNA and RNA from Escherichia coli BL 21 based on silica-coated magnetic nanoparticles. Sci China Chem. 2015;58(11):1774–8. https://doi.org/10.1007/s11426-015-5483-x.
45. Zhu QY, Xu YN, Qiu L, Ma CC, Yu BW, Song Q, et al. A scalable self-priming fractal branching microchannel net chip for digital PCR. Lab Chip. 2017;17(9):1655–65. https://doi.org/10.1039/C7LC00267J.
46. INTERNATIONAL STANDARD ISO 8655-2 (E), First edition. Piston-operated volumetric apparatus—part 2: piston pipettes. British Standards Institution; 2002.

Haowen Yang joined the deMello group as a research assistant at ETH Zurich in 2015. His research interests lie primarily in the field of microfluidics and nanotheranostics.

Zhu Chen is currently a lecturer at Hunan University of Technology. His research interest is molecular diagnostic systems.

Xiaobao Cao is currently a PhD student in the deMello group ETH Zurich, with a focus on microfluidics.

Zhiyang Li is the Head of the scientific research group in the Department of Clinical Laboratory at Nanjing Drum Tower Hospital. His research focuses on nanotechnology-based biomacromolecules for diagnosis and therapy, biochips and biosensors, and functional nanomaterials.

Stavros Stavrakis is currently a Senior Scientist in the deMello group in the Department of Chemistry and Applied Biosciences at ETH Zurich. His current research is focused upon developing new microfluidic/optofluidic platforms for single molecule enzymology, single-cell screening, high-throughput imaging flow cytometry, and fast enzyme kinetics using fluorescence lifetime detection.

Jaebum Choo has been in the faculty of the Bionano Engineering Department at Hanyang University since 1995. His current research programs are centered on the development of ultra-sensitive optical detection systems for rapid and accurate in vitro diagnostics.

Philip Howes is a Research Associate in the deMello group at ETH Zurich. His research focuses on the synthesis of biomolecular-nanoparticle conjugates and their application in biological sensing and imaging.

Andrew deMello is Professor of Biochemical Engineering in the Department of Chemistry and Applied Biosciences at ETH Zurich. His research interests cover a broad range of activities in the general area of microfluidics and nanoscale science, including the development of microfluidic devices for high-throughput biological and chemical analysis, ultrasensitive optical detection techniques, nanofluidic reaction systems for chemical synthesis, novel methods for nanoparticle synthesis, the exploitation of semiconducting materials in diagnostic applications, the development of intelligent microfluidics, and the processing of living organisms.

Nongyue He is a Professor in the School of Biological Science and Medical Engineering at Southeast University. His research interests are focused on biochips and biosensors, functional nanomaterials, controlled drug release, and tissue engineering.